

Hydraulics of the August 7, 1980, pyroclastic flow at Mount St. Helens, Washington

Alan H. Levine, Susan W. Kieffer

Department of Geology, Arizona State University, Tempe, Arizona 85287

ABSTRACT

Open-channel hydraulic theory for flow of an inviscid fluid down a channel of changing slope and width yields a longitudinal velocity profile that matches measured velocities of the August 7, 1980, pyroclastic flow at Mount St. Helens. The model is useful for prediction of zones of erosion, deposition, and hazards. It requires only topographic data, estimates of volumetric flow rate, and a Manning coefficient appropriate for the channel.

paper we have taken a new approach by applying hydraulic theory to demonstrate that channel geometry, not rheology, most strongly influenced the phenomena observed during the August 7 pyroclastic flow.

ASSUMPTIONS

We use steady open-channel hydraulic theory as summarized in the next section. Two of the simplifying assumptions need special emphasis because they are relevant to current concepts in volcanology. One assumption is that the fluid is inviscid and that material properties, such as particle concentration and viscosity, do not significantly influence the velocity variations in the channel. The second assumption is that observed flow-front velocity is approximately equivalent to a mean flow velocity calculated for steady conditions developed behind the flow front.

Conditions within volcanic flows—such as velocity, particle concentration, and mixture viscosity—have not been measured directly and must be inferred from interpretation of erosion surfaces or the flow deposits. Use of the term "pyroclastic flow" for the August 7 eruption im-

INTRODUCTION

The August 7, 1980, eruption at Mount St. Helens produced one of the best documented pyroclastic flows to date (Rowley et al., 1981; Hoblitt, 1986; Kuntz et al., 1990). Flow-front velocities varied by a factor of 6 along a path that included the steep, channelized "Stair Steps" and the unchannelized Pumice Plain (Figs. 1, 2). Sustained production of a cloud of elutriated ash occurred just below a sharp decrease in slope at the entrance to the Pumice Plain. Erosion was documented in the steep part of the channel. These observations provide a unique data set against which models of pyroclastic flows might be tested. To date, models proposed have focused on relations between the flow head and body (Hoblitt, 1986; Huppert et al., 1986) or on flow rheology (Wilson and Head, 1981; McEwen and Malin, 1989). In this

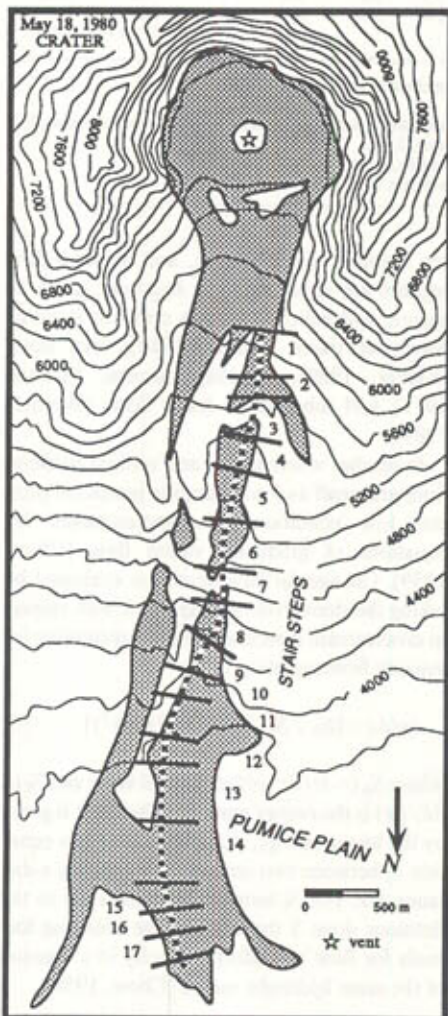


Figure 1. Topography of north side of Mount St. Helens and pumice deposits (shaded) from August 7, 1980, pyroclastic flow (after Kuntz et al., 1990). Dashed line indicates path of flow front; transverse bars are positions used by Hoblitt (1986) to calculate velocities over numbered reaches. For clarity, only 200 ft (61 m) contours are shown. Flow from crater was not visible until it had traveled 1.3 km to reach 1. Most deposits originated from flow down channel, including Stair Steps; small-volume flow, not considered in paper, left deposits east of Stair Steps.

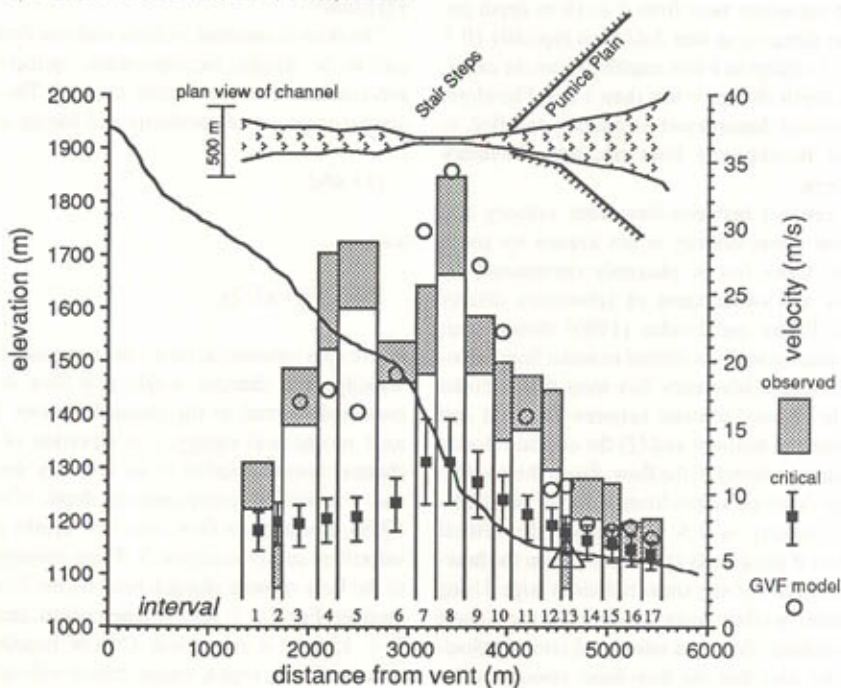


Figure 2. Observed velocities (shaded bars; Hoblitt, 1986), gradually varied flow (GVF) model velocities (circles), and calculated critical velocities (squares) in relation to channel slope and width. Vertical exaggeration for topography is 5.5 \times . Triangle in reach 13 represents calculated depth for subcritical flow if hydraulic jump was present (see text).

plies that the material is perceived to be a highly concentrated particulate system in which grain interactions are significant. However, relative volume fractions of solids and gas in these complex mixtures can vary with time or distance (Fisher, 1983). Particle concentrations may range from those characteristic of granular flow (as might be described by constitutive relations of Savage, 1979) to those characteristic of a dilute dusty gas (as might be described by pseudo-gas theory; Wallace, 1969). The analyses of the August 7 flow presented by Wilson and Head (1981) and McEwen and Malin (1989) assume characteristics nearer the granular-flow end member.

Viscosity is negligible in open-channel flow when (Thompson, 1972)

$$\Delta d / \Delta x \gg F^2 / Re, \quad (1)$$

where $\Delta d / \Delta x$ is the gradient of the flow depth, F is the Froude number ($F = u / \sqrt{gd}$, and Re is the Reynolds number ($Re = du / \nu$; u is mean velocity, g is acceleration due to gravity, ν is kinematic viscosity). Velocity and flow depth are coupled through the continuity equation. For observed velocities from 5 to 30 m/s and estimated flow depths from 3 to 10 m (Table 1), the Reynolds number is 10^3 to 10^5 (for plausible kinematic viscosities from 10^{-4} to 10^{-3} m²/s, Sparks, 1976; Wilson and Head, 1981). For calculated values of F from 1 to 5 (Table 1), the criterion for the inviscid flow approximation to be valid is then $\Delta d / \Delta x \gg 10^{-3}$ to 10^{-5} . Within the limits of the data, we find that flow-depth variations were from 1 to 10 m depth per 100 m distance, so that $\Delta d / \Delta x$ is typically 10^{-2} to 10^{-1} (except in a few reaches where the calculated depth change is less than 1 m). Therefore, the inviscid requirement is generally satisfied, as would be expected from the large Reynolds numbers.

A relation between flow-front velocity and internal mean velocity is not known for pyroclastic flows but is plausibly constrained by theory and observation of laboratory density flows. Britter and Linden (1980) showed that flow-front velocity is related to mean flow velocity through a buoyancy flux term that includes (1) the density contrast between the fluid and the ambient medium and (2) the critical velocity (discussed below) of the flow. From their analysis, for flows on slopes from 5° to 90°, the flow-head velocity is 1.5 ± 0.2 times the critical velocity if the density contrast between the flowing material and the ambient fluid is large. Using the observed flow-front velocities for the August 7 pyroclastic flow and calculated critical velocities, we find that the flow-head velocity is 2.0 ± 0.9 times the critical velocity, so we tentatively assume that we can apply the Britter and Linden (1980) results for the relations between flow-head and steady-flow velocity. They found that

TABLE 1. CHANNEL GEOMETRY DATA FOR HYDRAULIC CALCULATIONS

Reach number	Length	Elevation change	Width*	Relative width change $\Delta b / \Delta x$	Slope S_0 (°)	Velocity†		Depth‡	Froude‡	Total energy change ΔE (m)	Manning coef. estimate** n
						observed u (m/s)	critical u_c (m/s)				
1	280	34	180	-0.50	6.8	10.6	7.3	3.8	1.7		
2	90	11	200	0.22	6.9	5.5	8.0	9.7	0.6		
3	360	78	200	0.00	12.3	17.4	8.0	2.9	3.3	70.9	0.051
4††	200	39	150	-0.30	11.1	24.5	8.2	2.3	5.1	24.4	0.025
5	390	41	180	0.08	6.1	26.5	8.4	2.3	5.6	35.8	0.020
6††	390	68	50	-0.30	9.8	20.0	9.5	4.4	3.0	81.4	0.058
7	190	73	50	0.00	20.6	22.4	13.0	8.9	2.4	63.6	0.091
8	290	113	50	0.00	21.6	30.3	13.0	6.6	3.8	94.1	0.057
9	300	49	100	0.17	9.3	21.5	11.0	6.2	2.8	72.2	0.070
10	170	32	120	0.12	10.6	17.0	9.6	5.3	2.4	41.7	0.083
11	310	20	200	0.26	3.7	17.0	8.5	3.7	2.8	21.7	0.036
12	190	4	225	0.13	1.2	15.0	7.7	3.2	2.7	7.9	0.029
13††	120	7	300	0.63	3.5	5.4	7.2	7.1	0.6		
14	300	6	360	0.20	1.1	9.7	6.7	3.1	1.7	6.6	0.032
15	180	4	400	0.22	1.3	8.5	6.4	3.1	1.5	5.1	0.042
16	220	6	500	0.45	1.6	6.5	6.0	3.4	1.1	7.2	0.063
17	200	6	600	0.50	1.7	6.6	5.6	2.8	1.3	6.6	0.054
Avg. 0.049											

Note: All Δ values represent value at end of reach minus value at start of reach.

- * Measured from cross section at end of reach i .
- † Observed flow front velocities from Hoblitt (1986). Critical velocity, depth, and Froude number based on observed velocities.
- ‡ From equation 2; not evaluated for reaches of flow regime transition (2, 13).
- § From equation 5 for $S_f = \Delta E / \Delta x$. Average n weighted by reach length (Δx).
- †† Reaches in which relative width change strongly influenced the velocity; see Figure 3.

flow-head velocity is 60% of the mean steady-flow velocity behind the head. Our conclusion is that observed flow-front velocities are within a factor of two of mean steady-flow velocities. The uncertainty in the velocity measurements is comparable to this (Fig. 2), and we therefore compare calculated steady-flow velocities with measured flow-front velocities.

OPEN-CHANNEL HYDRAULIC THEORY

The flow is assumed to have uniform density and to be steady, incompressible, isothermal, and confined to a rectangular channel. The hydraulic equations of continuity and energy are

$$Q = ubd, \quad (2)$$

and

$$E = z + y + u^2 / 2g, \quad (3)$$

where Q is volumetric flow rate, u is mean flow velocity, b is channel width, d is flow depth measured normal to the channel bottom, E is total mechanical energy, z is elevation of the channel bottom relative to an arbitrary datum, and y is vertical component of depth (Chow, 1959). For a given flow rate, two depths (and velocities) satisfy equation 3. These correspond to the flow regimes characterized by the Froude number. For $F > 1$, flow is supercritical, and for $F < 1$, flow is subcritical. Critical conditions occur at $F = 1$, with a unique critical velocity.

$$u_c = (Qg/b)^{1/3}. \quad (4)$$

Transitions from supercritical to subcritical flow

are spatially discontinuous, and the two flow regimes are separated by a hydraulic jump. In nature, hydraulic jumps can occur as standing waves in rivers (Kieffer, 1985), lava flows (Kieffer, 1989), turbidity currents (Komar, 1971), and subaqueous debris flows (Weirich, 1989).

In reaches where lateral and vertical accelerations are small and no hydraulic jumps are present, low conditions are approximated by equations of gradually varied flow (Chow, 1959). Changes in flow depth are evaluated by taking the derivative of equation 3 with respect to downstream direction (x) and substituting for velocity from equation 2,

$$\partial y / \partial x = [S_0 - S_f] / [1 - Q^2 / (gb^2y^3)], \quad (5)$$

where $S_0 (= \partial z / \partial x)$ is the channel slope and $S_f (= \partial E / \partial x)$ is the energy gradient. The latter is given by the loss in energy, ΔE , evaluated from equation 3, between two sections separated by a distance Δx . The S_f term is also equivalent to the fictitious slope S that satisfies the Manning formula for flow of uniform velocity in a channel of the same hydraulic radius (Chow, 1959),

$$u = S^{1/2} R^{2/3} n^{-1}, \quad (6)$$

where n is the empirical Manning coefficient and R is the hydraulic radius (ratio of cross-section area to wetted perimeter). At a given flow rate, the regime (supercritical or subcritical) in a given channel section is determined by the ratio of the uniform flow velocity (equation 6) to the critical velocity (equation 4).

The Standard Step Method (Chow, 1959), a finite-difference approximation to equation 5, is

used to solve for depth as a function of distance in channels of variable width. The method requires a known control (boundary) condition. For a given discharge, either a measured depth or critical conditions must be specified at some location. In increments of Δx , calculations from this known control condition proceed upstream if the flow is subcritical and downstream if it is supercritical. Equations 4 and 5 are solved iteratively for the depth.

For the present analysis, changes in velocity (the measured parameter) are of more interest than changes in depth. Downstream-velocity variation, expressed as $1/u (\partial u/\partial x)$, is obtained from equation 5 and the derivative of equation 2,

$$\frac{1}{u} \frac{\partial u}{\partial x} = \frac{[1/b \partial b/\partial x + 1/y(S_0 - S_f)]}{[F^2 - 1]} \quad (7)$$

This form of the gradually varied flow formula illustrates that velocity changes are influenced by the sign and magnitude of (1) the Froude number, F ; (2) the downstream width variation, $1/b (\partial b/\partial x)$; and (3) the difference between channel slope and energy gradient ($S_0 - S_f$). Relations between these factors are summarized in a graph of the width term vs. the slope term of equation 7 (Fig. 3, discussed below).

APPLICATION OF HYDRAULIC THEORY

Channel geometry data (Table 1) were determined from topographic maps, aerial photographs (taken on September 9, 1980), distribution of pumice deposits (Kuntz et al., 1990), and photographs of the flow (Hoblitt, 1986). In the upper reaches, channel widths are well defined by cross sections that bracket the reaches of the observed velocity data (Fig. 1). On the Pumice Plain, an effective channel width was estimated from the distribution of pumice deposits (Fig. 2), but because the flow was relatively unconfined, the results should be interpreted with caution. Flow rate (Q) was obtained by two methods: (1) deposit volume, $4 \times 10^6 \text{ m}^3$ (Kuntz et al., 1990), divided by eruption duration, 6.5 min (Hoblitt, 1986), yields $\sim 10^4 \text{ m}^3/\text{s}$; (2) equation 2 applied for average values in the Stair Steps ($u = 20 \text{ m/s}$, $b = 50 \text{ m}$, $y = 10 \text{ m}$) also yields $\sim 10^4 \text{ m}^3/\text{s}$. Critical velocities calculated from equation 4 indicate that most observed flow-front velocities were supercritical (Table 1).

For the Standard Step Method, the x -step increment was 10 m. We used a Manning coefficient of $n = 0.05$, a typical value for rough-bed natural streams (Chow, 1959). Energy losses in each reach were calculated independently by applying equation 2 to each reach (Table 1) and by solving equation 5 for S . The results of the two methods are in good agreement for $n = 0.05$. Values of n less than 0.03 or greater than 0.07 yield velocities significantly different from those

observed. Lack of an upstream control point prevented modeling the flow in reaches 1 and 2. Because observed velocities passed from subcritical in reach 2 to supercritical in reach 3 (Fig. 2), critical flow conditions at the start of reach 3 were used as the upstream control for the series of channel sections from reach 3 down to the Pumice Plain. We chose to model supercritical flow through all reaches, and below we discuss the possibility of subcritical flow in reach 13.

The hydraulic model yields velocities that compare well with the observed velocities (Fig. 2), with exceptions in reaches 5 and 13. In defining the width of reach 5, we did not attempt to account for a large bedrock obstacle that is observable in aerial photographs and is reflected by the flow indicators mapped by Kuntz et al. (1990). The obstacle constricted part of the reach, and with a slope in excess of the energy gradient, it would have forced a local acceleration of the flow (this is not intuitive, but can be deduced by examining equation 7 and Fig. 3).

Observed flow-front velocities decreased from a supercritical $\sim 15 \text{ m/s}$ in reach 12 to a subcritical $\sim 5 \text{ m/s}$ in reach 13 (Fig. 2, Table 1). However, the calculated velocity in reach 13 is about 8 m/s , under the assumption used in the model that the flow remained supercritical. Hoblitt (1986) observed that at this location "the character of the flow front changed shortly after it moved onto the gently sloping pumice plain; the

convex, colloform ash clouds rose off the ground and were succeeded by a thin, light-colored wedge." Because velocities calculated with the assumption of supercritical flow are larger than those observed, we speculate that the observed behavior may reflect a transition from supercritical to subcritical flow, via a hydraulic jump generated by the decrease in slope from the Stair Steps to the Pumice Plain. Vertical accelerations that occur within a hydraulic jump (Chow, 1959) may have contributed to the ash clouds rising from the flow. Huppert et al. (1986) noted that it was peculiar that this velocity decrease occurred out on the Pumice Plain where the slope was gentle and uniform. However, hydraulic jumps occur downstream of slope inflections if the depth after the jump is low (Chow, 1959). For the flow front, the downstream depth was zero. Reach 13 is $\sim 600 \text{ m}$ downstream of the slope inflection, so the position of the proposed hydraulic jump is consistent with hydraulic theory.

Calculation of flow velocity on the downstream side of the hydraulic jump from conservation of momentum (Chow, 1959) yields a velocity of 5 m/s , in good agreement with the observed range of 3 to 8 m/s (Fig. 2). We suspect that subcritical flow was sustained only over a short distance entirely within reach 13 because observed velocities in downstream reaches 14–17 are supercritical. The modeling of

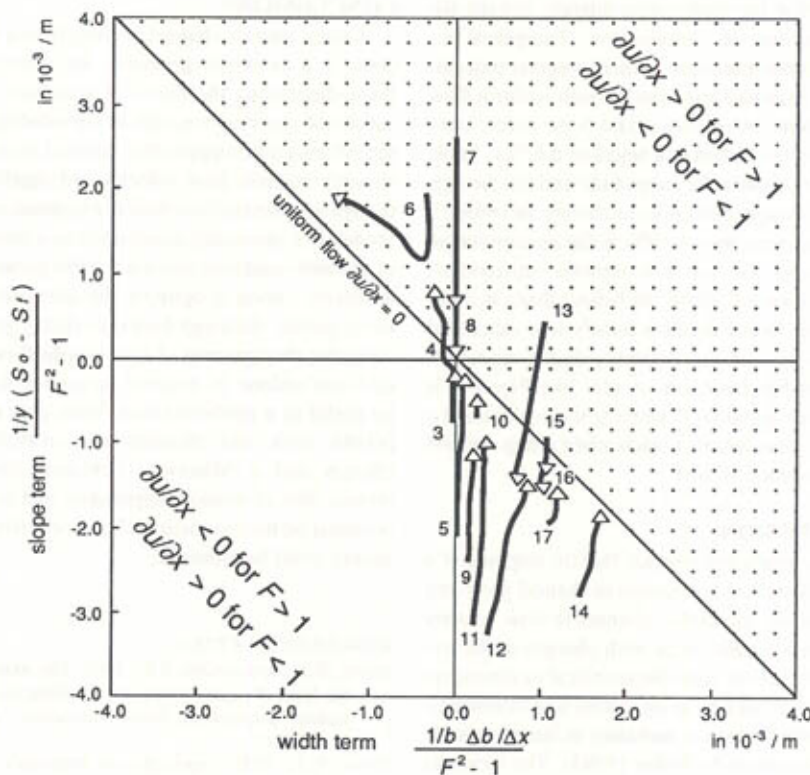


Figure 3. Trajectories of channel-width term vs. channel-slope term of equation 7 for results from Standard Step calculations. Variables defined in text. Discontinuities between trajectories reflect abrupt changes in channel slope, in some cases real and in others, an artifact of simplified geometry of constant-slope reaches.

transitions in flow regimes requires specifications of new control conditions. Because subcritical flow occurred only in the single reach 13 out on the Pumice Plain where application of a channelized flow model is tenuous, we did not attempt to model the flow transition. Measured velocities are averages over reaches that are typically more than 100 m in length, and we suspect that changes in flow properties and even flow regimes occur on a scale not resolvable in the data.

The influence of channel geometry on velocity is illustrated by a graph of the width vs. the slope terms of equation 7 for each 10-m increment calculated by the Standard Step Method (Fig. 3). Each line in Figure 3 represents the evolution of conditions expressed by the velocity derivative and includes width and slope changes from the top to the bottom of the reach (indicated by changes from tail to head of arrow). If the width and slope terms in equation 7 sum to zero, velocity is constant. This condition defines a diagonal line in Figure 3. The perpendicular distance from this line is a measure of departure from uniform flow and is proportional to the magnitude of the velocity change expressed by the left side of equation 7. Within either one of the fields separated by the line of uniform flow, the sign of the velocity derivative is fixed by the given flow regime.

In most reaches the rate of channel-width variation with downstream distance is sufficiently small that the trajectories migrate toward the diagonal line of uniform flow. Exceptions are easily spotted because of their irregular trajectories or because they cross through uniform flow conditions. In reaches 4 and 6 the severe constriction (expressed as a negative $\Delta b/\Delta x$, Table 1) caused either the magnitude and/or the sign of the velocity derivative to change. In reach 13 the trajectory drawn reflects the assumption in the model that the flow remains supercritical, but as discussed above, we believe that a hydraulic jump forced the flow locally to a subcritical regime, so that the trajectory drawn represents an unstable condition. A plot like Figure 3 is therefore useful for examining the evolution of a flow regime within a reach when a step method of calculation is used.

DISCUSSION

Our results demonstrate that the response of a pyroclastic flow to changes in channel geometry is complex; substantial changes in flow velocity and flow regime occur with changes in the terrain of the flow path. Supercritical to subcritical transitions may be as important flow-transformation phenomena as turbulent to laminar transitions discussed by Fisher (1983). The locations where flow rheology can be inferred, such as in deposits on the Pumice Plain (Wilson and Head, 1981), may not contain a record representative of the entire flow history.

The range of velocities, 5 to 30 m/s, suggests varying transport capacities in the flow and that erosional and depositional patterns could be complicated. Transport capacity criteria are not well established for pyroclastic flows, but for comparisons we note that water flowing at 10 m/s in the Colorado River is capable of moving boulders 1 m in diameter or larger. The estimated density in the pyroclastic flow is similar to that of water, and flow velocities were greater than 10 m/s for the entire steep section of the Stair Steps, where wall erosion and channel-bottom scour were documented by Rowley et al. (1981).

In pyroclastic-flow deposits, the velocity decrease through a hydraulic jump may be represented by an accumulation of large lithic clasts (Clark, 1984). Hydraulic jumps generated by slope inflections have been suggested as sources for lithic-rich units in pyroclastic flows at Laacher See in Germany (Freundt and Schmincke, 1985) and St. Kitts in the West Indies (Roobol et al., 1987). Although vertical sections of August 7 deposits near the Stair Steps have not been described, Rowley et al. (1981) described lag deposits of coarse pumice from a June 12 flow that decelerated at the base of a preexisting phreatic pit. The flow variations described in this study should be considered when interpreting spatial relations and facies in pyroclastic deposits.

CONCLUSIONS

A steep, narrow channel opening onto a wide plain is a common geometry for pyroclastic flows descending the flanks of volcanoes. The success of our simple model in reproducing observed velocities suggests that channel geometry strongly controls flow velocity and depth. Although an empirical coefficient n appears in our model, it is physically constrained as a measure of channel roughness and is not a free parameter arbitrarily varied to optimize the calculated velocity profile. Although hydraulic theory greatly simplifies the dynamics of a pyroclastic flow and does not address its material properties, it may be useful as a predictive tool. With only topographic data, and estimates of potential discharges and a Manning coefficient for the terrain, sites of erosion, deposition, and hazard potential on the channelized flanks of active volcanoes could be estimated.

REFERENCES CITED

- Britter, R.E., and Linden, P.E., 1980, The motion of the front of a gravity current travelling down an incline: *Journal of Fluid Mechanics*, v. 99, p. 531-543.
- Chow, V.T., 1959, *Open-channel hydraulics*: New York, McGraw-Hill, 680 p.
- Clark, S., 1984, The relevance of hydraulic jumps to pyroclastic flows [abs.]: *Eos (Transactions, American Geophysical Union)*, v. 65, p. 1142.

- Fisher, R.V., 1983, Flow transformations in sedimentary gravity flows: *Geology*, v. 11, p. 273-274.
- Freundt, A., and Schmincke, H.-U., 1985, Lithic-enriched segregation bodies in pyroclastic flow deposits of Laacher See Volcano (East Eifel, Germany): *Journal of Volcanology and Geothermal Research*, v. 25, p. 193-224.
- Hoblitt, R.P., 1986, Observations of the eruptions of July 22 and August 7, 1980, at Mount St. Helens, Washington: U.S. Geological Survey Professional Paper 1335, 44 p.
- Huppert, H.E., Turner, J.S., Carey, S.N., Sparks, S.J., and Hallworth, M.A., 1986, A laboratory simulation of pyroclastic flows down slopes: *Journal of Volcanology and Geothermal Research*, v. 30, p. 179-199.
- Kieffer, S.W., 1985, The 1983 hydraulic jump in Crystal rapid: Implications for river-running and geomorphic evolution in the Grand Canyon: *Journal of Geology*, v. 93, p. 385-406.
- , 1989, The relation of flow regimes to stratigraphy [abs.]: *New Mexico Bureau of Mines and Mineral Resources Bulletin* 131, p. 308.
- Komar, P.D., 1971, Hydraulic jumps in turbidity currents: *Geological Society of America Bulletin*, v. 82, p. 1477-1488.
- Kuntz, M.A., Rowley, P.D., and MacLeod, N.S., 1990, Geologic map of pyroclastic flow and related deposits of the 1980 eruptions of Mount St. Helens, Washington: U.S. Geological Survey Miscellaneous Investigations Map I-1950, 1:12,000.
- McEwen, A.S., and Malin, M.C., 1989, Dynamics of Mount St. Helens' pyroclastic flows, rockslide-avalanche, lahars, and blast: *Journal of Volcanology and Geothermal Research*, v. 37, p. 205-231.
- Roobol, M.J., Smith, A.L., and Wright, J.V., 1987, Lithic breccias in pyroclastic flow deposits on St. Kitts, West Indies: *Bulletin of Volcanology*, v. 49, p. 694-707.
- Rowley, P.D., Kuntz, M.A., and MacLeod, N.S., 1981, Pyroclastic-flow deposits: U.S. Geological Survey Professional Paper 1250, p. 489-512.
- Savage, S.B., 1979, Gravity flow of cohesionless granular materials in chutes and channels: *Journal of Fluid Mechanics*, v. 92, p. 53-96.
- Sparks, R.S.J., 1976, Grain size variations in ignimbrites and implications for the transport of pyroclastic flows: *Sedimentology*, v. 23, p. 147-188.
- Thompson, P.A., 1972, *Compressible-fluid dynamics*: New York, McGraw-Hill, 665 p.
- Wallace, G.B., 1969, *One-dimensional two-phase flow*: New York, McGraw-Hill, 408 p.
- Weirich, F.H., 1989, The generation of turbidity currents by subaerial debris flows, California: *Geological Society of America Bulletin*, v. 101, p. 278-291.
- Wilson, L., and Head, J.W., 1981, Morphology and rheology of pyroclastic flows and their deposits, and guidelines for future observations: U.S. Geological Survey Professional Paper 1250, p. 513-524.

ACKNOWLEDGMENTS

We thank R. Hoblitt (U.S. Geological Survey) for photographs of the August 7 eruption and P. Rowley (U.S. Geological Survey) for observations on the Stair Steps. P. Delaney, A. McEwen, J.-C. Komorowski, and an anonymous reviewer provided helpful comments. The ARCS Foundation granted a scholarship to Levine.

Manuscript received April 11, 1991
 Revised manuscript received July 5, 1991
 Manuscript accepted July 16, 1991